



HAL
open science

Multipath Mitigation Methods Based on Diversity Algorithms

Sébastien Rougerie, Gérald Carrié, Jonathan Israel, L. Ries, Michel Monnerat,
Paul Thevenon

► **To cite this version:**

Sébastien Rougerie, Gérald Carrié, Jonathan Israel, L. Ries, Michel Monnerat, et al.. Multipath Mitigation Methods Based on Diversity Algorithms. 26th International Technical Meeting of The Satellite Division of the Institute of Navigation (ION GNSS+ 2013), Sep 2013, Nashville, United States. hal-01353720

HAL Id: hal-01353720

<https://hal.science/hal-01353720>

Submitted on 12 Aug 2016

HAL is a multi-disciplinary open access archive for the deposit and dissemination of scientific research documents, whether they are published or not. The documents may come from teaching and research institutions in France or abroad, or from public or private research centers.

L'archive ouverte pluridisciplinaire **HAL**, est destinée au dépôt et à la diffusion de documents scientifiques de niveau recherche, publiés ou non, émanant des établissements d'enseignement et de recherche français ou étrangers, des laboratoires publics ou privés.

Multipath Mitigation Methods Based on Diversity Algorithms

S. Rougerie, *AUSY*

G. Carrie, *previously with ONERA, now with Thales Alenia Space France*

J. Israel, *ONERA*

L. Ries, *CNES*

M. Monnerat, *Thales Alenia Space France*

P. Thevenon, *previously with CNES, now with ENAC*

BIOGRAPHIES

Sebastien Rougerie graduated from ENAC (the French civil aviation school) with an engineer diploma and the Master of Science from the University of Toulouse in 2008. He received a Ph.D. degree in array processing in 2012 from ISAE Toulouse. Since then, he's working for AUSY, a consulting company in informatics based in Toulouse, in collaboration with ONERA and Thales Alenia Space

Guillaume Carrie graduated from ISAE, Toulouse, France, with an engineer diploma in aeronautics and a M.S. degree in signal processing in 2003 and a Ph.D. degree in array processing for GNSS receivers in 2006. From the end of 2006 to the end of 2007, he was with SILICOM, working on the development of GNSS receivers and simulators. From early 2008 to March 2013, he was with ONERA where he was responsible for research activities on propagation channel modeling. He led the development of technologies for GNSS receivers robust to propagation conditions and he was a French delegate at ITU-R SG3. Since April 2013 he is working as a research and development engineer at Thales Alenia Space France. His current research interests focus on GNSS receiver signal processing.

Jonathan Israel graduated for Télécom ParisTech, Paris, France, with an engineer diploma in signal processing and a Master of Science in Mathematics from the Ecole Normale Supérieure of Cachan in 2005. Since 2006, he has been working at ONERA. His fields of interest include physical statistical propagation channel characterization and signal processing for GNSS applications.

Lionel Ries is head of the localisation / navigation signal department in CNES, the French Space Agency. The department activities deal with signal processing, receivers and payload regarding localisation and navigation systems including GNSS (Galileo, GNSS space receivers), Search & Rescue by satellite

(SARSAT, MEOSAR), and Argos. He is also coordinating for CNES, research activities for future location / navigation signals, user segments equipments and payloads.

Michel Monnerat, location infrastructure manager within the technical direction of the Navigation and Integrated Communications Business Segment, Thales Alenia Space. After working on many radar and data collection programs within Alcatel Space, including being in charge of the onboard processing of the ARGOS/SARSAT payload, he has been involved in the Galileo program since 1998, particularly for the signal design and performance aspects. He is now in charge of the research and development for the ground location reinforcement solutions, as well as location standardization and innovative user equipment algorithms and hybridizations.

Paul Thevenon graduated as electronic engineer from Ecole Centrale de Lille in 2004 and obtained in 2007 a research master at ISAE in space telecommunications. In 2010, he obtained a Ph.D. degree in the signal processing laboratory of ENAC in Toulouse, France. From 2010 to 2013, he was employed by CNES, the French space agency, to supervise GNSS research activities and measurement campaigns. Since the July 2013, he is employed by ENAC as Assistant Professor. His current activities are GNSS signal processing, GNSS integrity monitoring and hybridization of GNSS with other sensors.

ABSTRACT

Multipaths (MP) are still one of the major error sources in Global Navigation Satellite Systems operating in challenging environments such as urban areas. This paper presents how diversity algorithms may improve the multipath mitigation performances. The diversity can either lie on the space domain (antenna diversity) or on the frequency domain (frequency band diversity). In both cases, the algorithms principle consists in taking benefit from information redundancy given by multiple diverse channels.

INTRODUCTION

In Global Navigation Satellite Systems (GNSS) applications, multipath (MP) errors are still one of the major error sources in conventional receivers. The additional signal replicas due to reflections introduce a bias in Delay Lock Loops (DLL), which finally leads to a positioning error. Several techniques have been developed for multipath mitigation or estimation. The most popular approach is the Narrow Correlator Spacing [1], which reduces the Chips spacing between two correlators in order to cut down the impact of multipath on the DLL. However, this technique suffers from high sensitivity to noise, and cannot mitigate short delay multipath (<0.1 Chips). Based on the Maximum Likelihood (ML) estimation, the Multipath Estimating Delay-Lock-Loop (MEDLL) [2] algorithm has also been proposed to estimate the delay and the power of all the paths by studying the shape of the cross correlation function. This approach shows better performance than the Narrow Correlator Spacing technique, but short delay multipath mitigation (<0.1 Chips) is still an issue. More recently, the use of diversity algorithms has been proposed for multipath mitigation. The diversity can either lie on the space domain (antenna diversity) or on the frequency domain (frequency band diversity). In both cases, the algorithms principle consists in taking benefit from information redundancy due to the use of diverse channels.

In the space domain, the redundant parameters are the time of arrival and the Doppler of the echoes and the diversity lies in the phase delays between antennas of an array. Actually, antenna array perform a spatial sampling of the wave front which makes possible the discrimination of the sources in the space domain (azimuth and elevation). As the time-delay domain and space domain can be assumed as independent, we can expect to mitigate/estimate very short delay multipaths by using an antenna array. However, since the array size, cost and complexity should be limited, we focus our study on small arrays with a small number of antennas: typically a 2×2 square array. In the frequency domain, the redundant parameters are the time of arrival of the echoes and the diversity is due to homothetic Doppler shifts and potentially to waveforms. Here, we focus on the frequency diversity, and not on the waveform diversity. Thus, we selected the GALILEO band E5a / E5b (BPSK(10) modulation) for this study.

The goal of this paper is to present an estimator based on the maximum likelihood theory which makes use of the diversity provided by an antenna array (multi-antenna processing) or by several GNSS frequencies (multi-frequency processing), in order to improve the multipath performances of a receiver. In a multi-antenna context, the algorithm and the associated performances have already been presented in [3], [4], [5] based on theoretical analysis and simulations. Recently, these results have been confirmed with real world data acquired

with the experimental device presented in [6]. This experimental validation is illustrated in this paper. In a multi-frequency context, the maximum likelihood algorithm has not yet been presented. This paper introduces this concept and presents simulation results which demonstrate the potential of multi-frequency processing for the multipath mitigation.

The paper is organized as follows: the signal model and the main assumptions are described in a multi-antenna and multi-frequency context in section 1. The estimators which use the space or frequency diversity in order to reject multipath are given in section 2. The section 3 presents the experimental results in the array processing context, and the section 4 proposed the simulation results in a multi-frequency context. Finally, in section 5, we present our conclusions and future work.

1. SIGNAL MODEL AND MAIN ASSUMPTIONS

1.1 Single Channel Signal Model

Let's assume we receive L_X narrowband planar wave fronts of wavelength λ_X , where X denotes one channel of the GNSS receiver (one antenna and one frequency). The one antenna, one frequency GNSS baseband signal can be denoted in the most general case:

$$z^X(t) = \sum_{l=0}^{L_X-1} [\gamma_l^X \exp(2j\pi\nu_l^X t) c^X(t - \tau_l^X)] + n^X(t) \quad (1)$$

where $\{\gamma_l^X, \tau_l^X, \nu_l^X\}_{l=0:L_X-1}$ are respectively the complex amplitude, time delay and Doppler shift of the l^{th} path associated to the channel X (the index $l=0$ corresponds to the LOSS), and $n^X(t)$ the additional complex white Gaussian noise of the channel X . Here, $c^X(t)$ denotes the Pseudo-Random-Noise (PRN) sequence of the considered GNSS signal. As we focus on the tracking performances, we do not take into account potential navigation message or secondary code. The code period is equal to $T = 1$ ms, a rectangular chip shape is assumed and the chip rate is denoted F_c .

Collecting the samples of the complex baseband signal leads to a $M \times N_{snap}$ matrix where N_{snap} denotes the number of Snapshots and M the number of channels ($M = N_{antenna} \times N_{freq}$). Typically, N_{snap} is larger than 200 000 (corresponding to a 20ms integration and a 10MHz sampling rate) and thus, a direct processing of the baseband signal with ML algorithms can hardly be implemented in real time. In order to compress the signal, we propose to use the scheme presented in the Fig. 1. For each channel, a bank of correlators is used to compress the signal and to get access to the relative delays of the sources, and the post correlation time taps enable to get access to the Doppler domain. This array is then defined by 4 parameters: the number M of channels, the number N of post-correlation Taps, the number P of correlators, and

the time spacing C_s between the correlators. Note that the sampling time of the post-correlated signal is equal to T_{int} . Therefore, we get the following relation between the number of raw snapshots and the number of post-correlated Taps: $N_{snap} = N \times T_{int} \times f_s$ where f_s is the sampling rate of the baseband signal. At the output of the compression step proposed in Fig. 1, the signal model for the channel X can be written as ([3], [4], [5]):

$$\mathbf{x}^X = \sum_{l=0}^{L_X-1} [\tilde{\gamma}_l^X \tilde{\mathbf{r}}_C^X(\tau_{rl}^X, \nu_{rl}^X)] + \mathbf{n}_{pc}^X \quad (2)$$

where \mathbf{n}_{pc}^X is the output noise which is assumed iid between each channel in this paper, $\tilde{\gamma}_l^X$ denotes the post correlated complex amplitude of the path indexed by l , and the vector $\tilde{\mathbf{r}}_C^X(\tau_{rl}^X, \nu_{rl}^X)$ is the result of the concatenation of:

- the outputs of the P correlators arranged in a column vector resulting in a sampled cross-correlation function,
- the N cross-correlation functions arranged in a column vector which capture the temporal evolution of the post-correlation signal.

From [3], [4], [5], we have the following relations:

$$\tilde{\mathbf{r}}_C^X(\tau_{rl}^X, \nu_{rl}^X) = \mathbf{e}(\nu_{rl}^X) \otimes \mathbf{r}^X(\tau_{rl}^X) \quad (3)$$

with

$$\mathbf{r}^X(\tau_{rl}^X) = \left[r^X\left(\tau_{rl}^X - \frac{(P-1)C_s}{2}\right) \cdots r^X\left(\tau_{rl}^X + \frac{(P-1)C_s}{2}\right) \right]_{P \times 1}^T \quad (4)$$

$$\mathbf{e}(\nu_{rl}^X) = \left[1 \cdots \exp(2j\pi\nu_{rl}^X(N-1)T_{int}) \right]_{N \times 1}^T \quad (5)$$

where \otimes denotes the Kronecker product, $r^X(\cdot)$ is the correlation function of the PRN of the channel X , and we introduce the relative delay $\hat{\tau}^X$ and the relative Doppler $\hat{\nu}^X$ of the local replica with respect to the l^{th} path parameters: $\tau_{rl}^X = \hat{\tau}^X - \tau_l^X$, $\nu_{rl}^X = \hat{\nu}^X - \nu_l^X$. The space or frequency diversity is obtained with the concatenation of the channels, banks of correlators and post-correlation taps outputs in a $M \times N \times P$ column vector:

$$\mathbf{x} = \left[\mathbf{x}^{X1} \cdots \mathbf{x}^{XM} \right]_{MNP \times 1}^T \quad (6)$$

$$\mathbf{n}_{pc} = \left[\mathbf{n}_{pc}^{X1T} \cdots \mathbf{n}_{pc}^{XMT} \right]_{MNP \times 1}^T \quad (7)$$

1.2 Multi-Antenna Signal Model

In a multi-antenna context, each channel represents one antenna. During the experimental campaign (see section 3), we used a 2x2 square array, the antenna spacing was $\lambda/2$ ($M = 4$). The GPS C/A signals have been collected. The chip rate is therefore $F_c = 1.023\text{MHz}$ for the multi-antenna processing, and the cross correlation functions are identical for all the channels ($r^X = r, \forall X$).

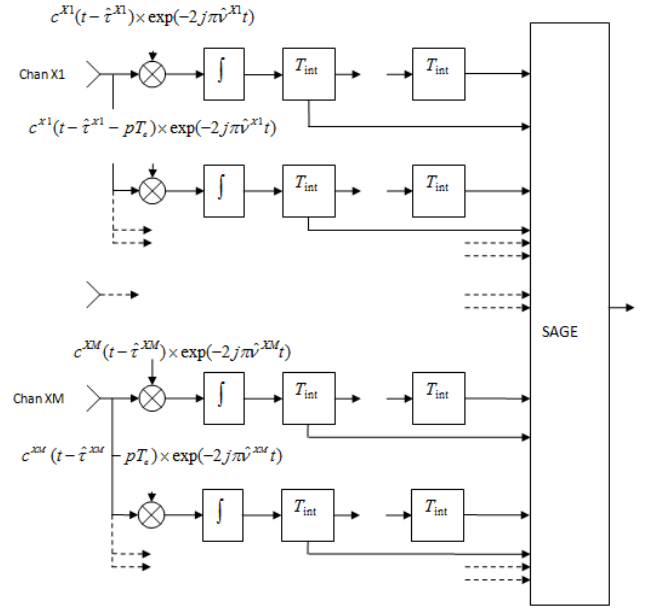


Fig. 1: Banks of correlators

Assuming an array with perfectly matched channels (no mutual coupling and the same RF transfer function whatever the channels, section 3), we get the following statements:

- the number of echoes are the same on each antenna $L_X = L, \forall X$,
- the delay and the Doppler of the echoes are identical on each channel ([3], [4], [5]),
 $\tau_{rl}^X = \tau_{rl}, \nu_{rl}^X = \nu_{rl}, \forall X$,
- the phase delays between each antenna can be modeled as [3] [4] [5]:

$$\left[\tilde{\gamma}_l^{X1} \cdots \tilde{\gamma}_l^{XM} \right]_{M \times 1}^T = \tilde{\gamma}_l \mathbf{a}(\theta_l, \varphi_l) \quad (8)$$

where $\mathbf{a}(\theta, \varphi)$ represents the steering vector and θ_l, φ_l the elevation and azimuth of the l^{th} path.

Finally, the signal model associated to an antenna array can be written as:

$$\mathbf{x} = \sum_{l=0}^{L-1} \mathbf{x}_l(\tilde{\gamma}_l, \theta_l, \varphi_l, \tau_{rl}, \nu_{rl}) + \mathbf{n}_{pc} \quad (9)$$

$$\mathbf{x}_l(\tilde{\gamma}_l, \theta_l, \varphi_l, \tau_{rl}, \nu_{rl}) = \tilde{\gamma}_l \mathbf{a}(\theta_l, \varphi_l) \otimes \tilde{\mathbf{r}}_C(\tau_{rl}, \nu_{rl}) \quad (10)$$

1.3 Multi-Frequency Signal Model

In the multi-frequency context, each channel represents one GNSS frequency. In order to focus on the multi-frequency processing (while avoiding multi-modulation processing), we use the GALILEO signal E5a / E5b with a BPSK(10) modulation ($M = 2$ and $X = E5a$ or $X = E5b$). Moreover, we use only the pilot component of the E5 signals, and the secondary code is assumed perfectly synchronized. With such hypothesis, the cross-correlation

functions are identical for each channel ($r^X = r \forall X$), and the chip rate is $F_c = 10.23\text{MHz}$.

In order to build a ML estimator which uses redundancies in the frequency domain, we need a multi-frequency model of the multipath. Based on experimental power measurements, [7] assumes that multipath on Galileo E5a and E5b bands are independent. Therefore, the outputs of correlators on both frequency bands can be considered as any independent statistical variables and they can be averaged right before the discriminator computation. By contrast, [8] considers that purely deterministic relationships exist between the wideband channel parameters and the authors propose a particle filtering approach which takes advantage of this information redundancy to improve the estimation of the direct path propagation delay. Based on asymptotic electromagnetic methods and ray bouncing, the GNSS multifrequency urban channel was analysed from the lower part to the upper part of the GNSS L-Band in [9] and [10]. These analyses showed on the one hand that the narrowband channels are independent between two GNSS frequency bands. But on the other hand, these analyses showed that even if the relations are not purely deterministic, a strong correlation exists between the wideband channel parameters (i.e. the delay, Doppler and direction of arrival parameters) [9] [10]. Based on this wideband point of view of the multi-frequency channel, we propose the following multipath model:

- The number of multipath are assumed to be identical for all the frequencies $L_X = L, \forall X$
- The Doppler shifts have an homothetic relation between the two bands

$$v_{rl}^{E5a} = v_{rl}^{E5b} \frac{\lambda_{E5b}}{\lambda_{E5a}}, \forall l \in [0, L-1]$$
- The delays are shifted between the two bands by a parameter independent of the path index "l":

$$\tau_{rl}^{E5a} = \tau_{rl}^{E5b} + \Delta_{E5a}^{E5b}, \forall l \in [0, L-1]$$
- No assumption is made on the complex amplitudes $\tilde{\gamma}_l^{E5a}, \tilde{\gamma}_l^{E5b}$.

The parameters Δ_{E5a}^{E5b} corresponds to the delay between the E5a band and the E5b band. This delay is due to the ionospheric delay which is frequency dependent, and to the RF group delays. The resulting multi-frequency signal model is therefore:

$$\mathbf{x} = \sum_{l=0}^{L-1} \begin{bmatrix} \tilde{\gamma}_l^{E5a} \tilde{\mathbf{r}}_C(\tau_{rl}, v_{rl}) \\ \tilde{\gamma}_l^{E5b} \tilde{\mathbf{r}}_C\left(\tau_{rl} + \Delta_{E5a}^{E5b}, v_{rl} \frac{\lambda_{E5a}}{\lambda_{E5b}}\right) \end{bmatrix}_{MNP \times 1} + \mathbf{n}_{pc} \quad (11)$$

$$\mathbf{x} = \sum_{l=0}^{L-1} \tilde{\mathbf{R}}_C(\tau_{rl}, \Delta_{E5a}^{E5b}, v_{rl}) \tilde{\boldsymbol{\gamma}}_l + \mathbf{n}_{pc}$$

where $\tau_{rl} = \tau_{rl}^{E5a}, v_{rl} = v_{rl}^{E5a}$ denote the relative delay and the relative Doppler shift associated to the E5a band, and

$$\tilde{\mathbf{R}}_C(\tau_{rl}, \Delta_{E5a}^{E5b}, v_{rl}) = \begin{bmatrix} \tilde{\mathbf{r}}_C(\tau_{rl}, v_{rl}) & \mathbf{0}_{NP \times 1} \\ \mathbf{0}_{NP \times 1} & \tilde{\mathbf{r}}_C\left(\tau_{rl} + \Delta_{E5a}^{E5b}, v_{rl} \frac{\lambda_{E5a}}{\lambda_{E5b}}\right) \end{bmatrix}_{NP \times M} \quad (12)$$

$$\tilde{\boldsymbol{\gamma}}_l = \begin{bmatrix} \tilde{\gamma}_l^{E5a} & \tilde{\gamma}_l^{E5b} \end{bmatrix}_{M \times 1}^T \quad (13)$$

2. MAXIMUM LIKELIHOOD ALGORITHM

2.1 Principle and SAGE / STAP Multi-Correlators Algorithm

We want to estimate a set of parameters denoted $\{\boldsymbol{\Psi}_l\}_{l \in [0, L-1]}$ for each path indexed by 'l'. The estimation of L (the number of echoes + LOSS) is not discussed in this study. Usually, L is fixed to a value large enough to capture all the dominant impinging waves. Classical information theory methods for model selection like Akaike's and Rissanen's [11] criteria can be used to estimate L . The ML estimation is given by $\hat{\boldsymbol{\Psi}} = \arg \max_{\boldsymbol{\Psi}} p(\mathbf{x}; \boldsymbol{\Psi})$, with \mathbf{x} the signal model at the output of the Taps-multicorrelators architecture (Fig. 1), and $p(\mathbf{x}; \boldsymbol{\Psi})$ the likelihood function:

$$p(\mathbf{x}; \boldsymbol{\Psi}) = \frac{1}{\pi^{NPM}} \frac{\exp(-[\mathbf{x} - \mathbf{x}_{si}(\boldsymbol{\Psi})]^H \boldsymbol{\Sigma}_{pc}^{-1} [\mathbf{x} - \mathbf{x}_{si}(\boldsymbol{\Psi})])}{\det \boldsymbol{\Sigma}_{pc}} \quad (14)$$

where $\mathbf{x}_{si}(\boldsymbol{\Psi}) = \sum_{l=0}^{L-1} \mathbf{x}_l(\boldsymbol{\Psi}_l)$ contains the superimposition of the post-correlation signals. $\boldsymbol{\Sigma}_{pc}$ denotes the covariance matrix of the post-correlation noise. The noise is no longer white after the correlation step [5], [12]. However, assuming the noise iid between the channels (between the antennas and between the GNSS frequencies) the post-correlation noise covariance matrix can be written as a bloc diagonal matrix:

$$\boldsymbol{\Sigma}_{pc} = E(\mathbf{n}_{pc} \mathbf{n}_{pc}^H) = \begin{bmatrix} \tilde{\sigma}_{X1}^2 (\mathbf{I}_N \otimes \boldsymbol{\Sigma}_{P,X1}) & \mathbf{0}_{NP} & \dots & \mathbf{0}_{NP} \\ \vdots & \ddots & & \\ \mathbf{0}_{NP} & & \tilde{\sigma}_{XM}^2 (\mathbf{I}_N \otimes \boldsymbol{\Sigma}_{P,XM}) & \\ & & & \end{bmatrix}_{MNP} \quad (15)$$

where $\tilde{\sigma}_X^2$ denotes the noise power after the correlation step for the channel X , and $\boldsymbol{\Sigma}_{P,X}$ is the correlation matrix of the PRN [3], [4], [5] and [12]. Considering the hypothesis made in section 1 (same noise power and same waveform on each channel whatever the diversity mode) the covariance matrix can be simplified in:

$$\boldsymbol{\Sigma}_{pc} = E(\mathbf{n}_{pc} \mathbf{n}_{pc}^H) = \tilde{\sigma}^2 (\mathbf{I}_{MN} \otimes \boldsymbol{\Sigma}_P) \quad (16)$$

The direct maximization of the likelihood function is a computationally prohibitive task since there is no

analytical solution. Moreover, $p(\mathbf{x}; \Psi)$ is generally not a concave function of Ψ , and L is usually high. In order to perform this optimization, we use the iterative process of the SAGE (Space-Alternating Generalized Expectation maximization) algorithm [13]. The basic concept of the SAGE algorithm is to use a hidden data space. Instead of estimating the parameters of all impinging waves in one search, the SAGE algorithm sequentially estimates the parameters of each signal. Thus, the SAGE algorithm breaks down the multi-dimensional optimization problem into several smaller problems.

However, prior to apply the SAGE methodology, we need to define admissible data space. We remind hereafter the corresponding definitions ([5], [13], [14]):

Definition 1 [13]: a set S is defined to be an index set if $S \neq \emptyset$, $\dim(S) \in [1, \dots, \dim(\Psi)]$, and S has no repeated entries. \bar{S} denotes the complement of S .

Definition 2 [13]: one iteration of the SAGE algorithm is defined as a full update of all the parameters of the parameter vector $\hat{\Psi}$. A full update of $\hat{\Psi}$ is achieved by sequentially conditioning on a sequence of subsets of parameters Ψ_S while keeping the parameters of the related complement subsets $\Psi_{\bar{S}}$ fixed.

Definition 3 [13]: a random matrix \mathbf{x}_S with a probability density function $p(\mathbf{x}_S; \Psi)$ is an admissible hidden data space with respect to Ψ_S for $p(\mathbf{x}; \Psi)$ if and only if the joint density of \mathbf{x}_S and \mathbf{x} satisfies:

$$p(\mathbf{x}, \mathbf{x}_S; \Psi) = p(\mathbf{x}, \mathbf{x}_S; \Psi_S) p(\mathbf{x}_S; \Psi) \quad (17)$$

The conditional density of \mathbf{x} given \mathbf{x}_S depends just on $\Psi_{\bar{S}}$, but not on Ψ_S . In other words, all the information related to the parameters Ψ_S in \mathbf{x} is included in \mathbf{x}_S .

2.2 SAGE / STAP Multi-Correlators in a Multi-Antenna Context

In the multi-antenna context, we use the signal model in (9) and (10). The set of parameters estimated by the ML algorithm is $\Psi_l = [\tilde{\gamma}_l, \theta_l, \varphi_l, \tau_{rl}, \nu_{rl}]^T, l \in [0, L-1]$. In order to solve the optimization problem [5] and [14] showed that the random matrix $\mathbf{x}_l(\tilde{\gamma}_l, \theta_l, \varphi_l, \tau_{rl}, \nu_{rl}) + \mathbf{n}_{pc,l}$ is an admissible hidden data space (with the convergence parameters $\beta_l=1$). Thus, we can apply the SAGE methodology to solve the optimization problem.

The first step of the SAGE algorithm, the so-called Expectation Step (E-STEP), consists in estimating the hidden data space with:

$$\hat{\mathbf{x}}_l = \mathbf{x} - \sum_{\substack{l'=0 \\ l' \neq l}}^{L-1} \mathbf{x}_{l'}(\Psi_{l'}) \quad (18)$$

The second step, the so-called Maximization Step (M-STEP), carries out the maximization of the log-likelihood function which is associated with the estimated hidden data space. In the case of the STAP multicorrelator signal, the reduced likelihood function (due to the linear relation between $\tilde{\gamma}_l$ and the signal model) to maximize is ([3], [4], [5]):

$$\tilde{\Lambda}(\Psi_l) = \frac{[\mathbf{a}^H(\theta_l, \varphi_l) \otimes \tilde{\mathbf{r}}_C^H(\tau_{rl}, \nu_{rl})] \hat{\mathbf{x}}_l}{M \times \tilde{\mathbf{r}}_C^H(\tau_{rl}, \nu_{rl}) \tilde{\mathbf{r}}_C(\tau_{rl}, \nu_{rl})} \quad (19)$$

$$\hat{\tilde{\gamma}}_l = \frac{[\mathbf{a}(\hat{\theta}_l, \hat{\varphi}_l) \otimes \tilde{\mathbf{r}}_C(\hat{\tau}_{rl}, \hat{\nu}_{rl})]^H \hat{\mathbf{x}}_l}{M \times \tilde{\mathbf{r}}_C^H(\hat{\tau}_{rl}, \hat{\nu}_{rl}) \tilde{\mathbf{r}}_C(\hat{\tau}_{rl}, \hat{\nu}_{rl})} \quad (20)$$

where $\tilde{\mathbf{r}}_C^H(\tau_{rl}, \nu_{rl})$ is given by ([3], [4], [5]):

$$\tilde{\mathbf{r}}_C^H(\tau_{rl}, \nu_{rl}) = \tilde{\mathbf{r}}_C^H(\tau_{rl}, \nu_{rl}) [\mathbf{I}_N \otimes \Sigma_P^{-1}] \quad (21)$$

2.3 SAGE / STAP Multi-Correlators in a Multi-Frequency Context

In the multi-frequency context, we use the signal model (11). However, it is harder to define admissible hidden data space for the SAGE algorithm. Indeed, let us propose three sets of parameters to estimate:

- 1) $\Psi_l = [\tilde{\gamma}_l^{ESa}, \tilde{\gamma}_l^{ESb}, \tau_{rl}, \nu_{rl}, \Delta_{ESa}^{ESb}]^T, l \in [0, L-1]$
- 2) $\Psi_0 = [\tilde{\gamma}_0^{ESa}, \tilde{\gamma}_0^{ESb}, \tau_{r0}, \nu_{r0}, \Delta_{ESa}^{ESb}]^T, \Psi_{0 < l < L} = [\tilde{\gamma}_l^{ESa}, \tilde{\gamma}_l^{ESb}, \tau_{rl}, \nu_{rl}]^T$
- 3) $\begin{cases} \Psi_l = [\tilde{\gamma}_l^{ESa}, \tau_{rl}^{ESa}, \nu_{rl}^{ESa}]^T, l \in [0, L-1] \\ \Psi_l = [\tilde{\gamma}_l^{ESb}, \tau_{rl}^{ESb}, \nu_{rl}^{ESb}]^T, l \in [L, 2L-1] \end{cases}$

The first proposition does not match with the definition 2 in section 2.1. Indeed, the parameter Δ_{ESa}^{ESb} appears in the definition of all the Ψ_l . Thus, in the sequential optimization process of SAGE, the set of parameters $\Psi_{l' \neq l}$ are note fixed.

For the second proposition, it is difficult to find an admissible hidden data space (definition 3). Indeed, if we use the data space $\tilde{\mathbf{R}}_C(\tau_{rl}, \Delta_{ESa}^{ESb}, \nu_{rl}) \tilde{\gamma}_l + \mathbf{n}_{pc,l}$, the set of parameters Ψ_l does not include all the information of the hidden data space for $l > 0$.

The last proposition matches with the definitions. However, this is equivalent to a mono channel SAGE estimation on each band and thus, we lose the redundancy brought by the multi-frequency multipath wideband channel model in [10].

The problem is due to the parameter Δ_{E5a}^{E5b} which appears in the definition of all the paths. We propose here to exclude this interband delay estimation from the ML optimization problem. In the case of the E5a / E5b processing, the ionospheric delays are very close and we can use a single RF stage. Thus, the assumption $\Delta_{E5a}^{E5b} = 0$ looks quite reasonable. However, in the case of the processing of other GNSS bands (E1 / E5 / E6), this simplification will not hold any more. Note however that the ionospheric and RF delays are phenomenon with very low dynamics. Thus, we can expect to build an estimator of Δ_{E5a}^{E5b} with longer integration time (more than 1min), robust to the multipath (see the example on Fig. 2).

From the ML point of view, the set of parameters to estimate for each path is now $\Psi_l = [\tilde{\gamma}_l^{E5a}, \tilde{\gamma}_l^{E5b}, \tau_{rl}, \nu_{rl}]^T, l \in [0, L-1]$. We can therefore use the SAGE methodology to solve the ML optimization problem where the reduced likelihood function for each hidden data space is:

$$\tilde{\Lambda}(\Psi_l) = \sum_{X=E5a, E5b} \left[\frac{|\tilde{\mathbf{r}}_C^H(\tau_{rl} + \Delta_{E5a}^X, \nu_{rl}, \lambda_X / \lambda_{E5a}) \tilde{\mathbf{k}}_l^X|^2}{\tilde{\mathbf{r}}_C^H(\tau_{rl} + \Delta_{E5a}^X, \nu_{rl}, \lambda_X / \lambda_{E5a}) \tilde{\mathbf{r}}_C(\tau_{rl} + \Delta_{E5a}^X, \nu_{rl}, \lambda_X / \lambda_{E5a})} \right] \quad (22)$$

$$\hat{\tilde{\gamma}}_l^X = \frac{|\tilde{\mathbf{r}}_C^H(\hat{\tau}_{rl} + \Delta_{E5a}^X, \hat{\nu}_{rl}, \lambda_X / \lambda_{E5a}) \tilde{\mathbf{k}}_l^X|}{\tilde{\mathbf{r}}_C^H(\hat{\tau}_{rl}, \hat{\nu}_{rl}, \lambda_X / \lambda_{E5a}) \tilde{\mathbf{r}}_C(\hat{\tau}_{rl}, \hat{\nu}_{rl}, \lambda_X / \lambda_{E5a})}, X = E5a, E5b \quad (23)$$

2.4 Implementation in a GNSS Receiver

To implement the SAGE / STAP algorithm in a GNSS receiver, we propose the architecture illustrated on Fig. 2. The multicorrelator array in Fig.1 is used in order to compress the data for all the channels. Afterward, we use the SAGE algorithm to solve the maximum likelihood problem, and the relative delay and Doppler estimations τ_{r0}, ν_{r0} are used to drive the DLL and FPLL. The key idea of our solution is to substitute the SAGE / STAP estimation to the conventional DLL and PLL / FLL discriminators [5].

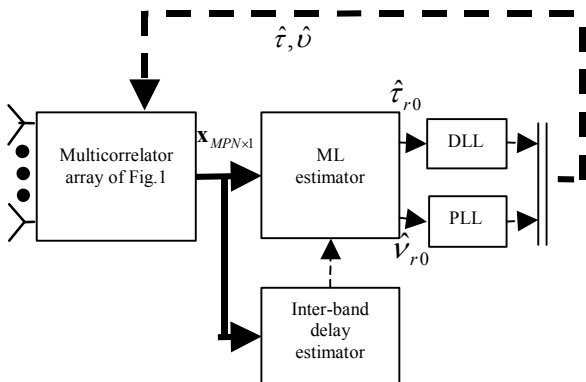


Fig. 2: Proposed receiver architecture

3. EXPERIMENTAL RESULTS IN A MULTI-ANTENNA CONTEXT

In a multi-antenna context, the algorithm and the associated performances have already been presented in [3], [4] and [5] based on numerical simulations. Here, we present the experimental results obtained with the CNES multi-antenna Bit Grabber [6]. The sensors of the antenna array were configured in a 2x2 square array ($\lambda/2$ spaced), and the frequency down conversion was selected in order to process the GPS C/A signal.

For the antenna array calibration, we used a spectrum analyzer in an anechoic chamber in order to characterize the four RF chains. Then, Finite Impulse Response (FIR) equalizers have been implemented in order to get a wide band compensation of the RF distortion [5]. The mutual coupling matrix was also measured (thanks to the scattering S_{ij} parameters [5]), and the coupling coefficients were lower than -20dB. Thus, in the case of GPS signal (which can be assumed as a narrow band signal from the antenna array point of view), the mutual coupling can be neglected [15].

The baseband signal was grabbed on a 34.375MHz bandwidth with 2 quantization bits. A software GPS C/A receiver has been implemented in MATLAB© and consists in signal acquisition, synchro-bit and tracking units. In the single antenna – single frequency case, the tracking step is based on classical DLL / PLL in order to estimate the pseudo-range and Phase/Doppler of the LOSS [16]. The DLL and the PLL are respectively based on a second and a third order loops, with a 1Hz and 10Hz bandwidth. The DLL is controlled with an Early Minus Late Discriminator (EMLD) with a 0.5 chip spacing between the early and the late correlators [16]. The PLL discriminator is an “atan2” [16]. In the multi-antenna case, the software allows to use beamforming algorithms (space filtering of the post correlated complex samples [5]). [4] and [5] propose a discussion on the choice of the appropriate beamformer when multipath occur. Then, we use here the “Conventional Beamforming Filter” (CBF) which consists in increasing the gain in the LOS direction. The software proposes also to use the SAGE / STAP algorithms in order to drive the tracking loops as in Fig. 2.

The antenna array and the bit grabber were mounted in a car (see Fig. 3) for mobile measurement in the city of Toulouse in France.



Fig. 3: Bit Grabber (left) and antenna array (right) mounted on a car.

We present here the results associated with two scenarios: one in a rural condition (sub-section 3.1) and one in an urban condition (sub-section 3.2).

For the evaluation of the tracking performance of the DLL, we propose to use the pseudo range compensated by integrated Doppler (also called CCD for Carrier Code Difference). The integrated Doppler (i.e. the signal unwrapped phase) is widely used for ultra precise applications. When the integer cycle count ambiguity is resolved, this measurement is equivalent to a pseudo-range measurement with an accuracy better by two orders of magnitude than the conventional accuracy of pseudo-range measurement based on the code delay [16]. When there is no multipath, the CCD is centred around the null value. When multipath exist, the phase and the code are affected in different proportions. That is breaking down the code-carrier coherency. Hence, a smaller value of the pseudo-ranges compensated by the integrated Doppler indicates a better time delay estimation in multipath conditions. We propose the following indicator:

$$\begin{aligned}\psi(t) &= PR(t) + \lambda \int_{u=0}^t f_d(u) du \\ \tilde{\psi}(t) &= \psi(t) - \psi(0)\end{aligned}\quad (24)$$

where $PR(t)$ denotes the pseudo-range estimated from the DLL code delay, and $f_d(t)$ the Doppler shift estimated from the PLL. As we do not solve the cycle counts ambiguity, we subtract $\psi(0)$ in order to initialize the CCD indicator to zero.

3.1 Results in a Rural Environment

The first environment is illustrated on the Fig. 4. The car is moving at 50km/h on a tree sided road. In most of the cases, the receiver is in clear sky situation. However, some fading events can occur due to the vegetation along the road. The Fig. 5 represents the $\tilde{\psi}(t)$ value and the estimated C/N_0 for the PRN25 (elevation 63°), in the cases of the mono-antenna tracking, tracking augmented with a CBF, and tracking driven by the SAGE / STAP algorithms. After a transition step of 5s, the multi-antenna processing (CBF and SAGE /STAP) improves the C/N_0 by 6dB as expected, and we observe a reduction of the standard deviation of the CCD $\tilde{\psi}(t)$. The processing was done on 10min of signal, and 6 satellites were tracked. In order to compare the performances of each algorithm, we compute the standard deviation $\sigma = std(\tilde{\psi}(t))$ for each satellite and for each processing algorithm. The table 1 summarizes for each algorithm the average values of σ on all the tracked satellites.

Here, the antenna diversity improves the DLL tracking performances by a factor of 1.5 in the case of the CBF, and by more than a factor of 4 in the case of the SAGE / STAP algorithms. It shows that multi-antenna methods improve strongly the tracking performances in terms of pseudo-range estimation.



Fig. 4: Rural environment

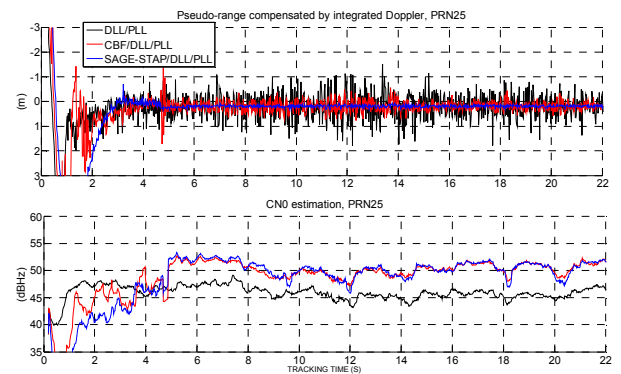


Fig. 5: Pseudo range compensated by integrated Doppler (CCD) and C/N_0 for the PRN 25 in rural environment

Table 1: standard deviation of the CCD averaged on all the tracked satellites in a rural environment

Algorithms	σ (m)
DLL/PLL	6.2
CBF/DLL/PLL	4.3
SAGE/DLL/PLL	0,45

3.2 Results in an Urban Environment

The second scenario corresponds to an urban environment as illustrated in Fig. 6. The car is moving slower than 6km/h in an urban canyon. The scenario presents a high multipath activity, with many fading events due to buildings, cars or trees. The Fig. 7 present the results for the PRN 29 (elevation 65°), and the table 2 summarizes the average σ values obtained for 2 satellites during 1min.

In this scenario, the single antenna approach loses the tracking lock. The CBF approach does not track correctly due to the difficulty in estimating the LOS DOA in presence of severe multipath conditions. However, the SAGE / STAP algorithm is able to track the LOS signal as expected in [3], [4], [5] and [6]. It is interesting to note that the improvement is better than a factor of 4 compared to the single antenna approach. It shows that the proposed algorithm reduces not only the error due to the noise, but also the error due to multipath.



Fig. 6: Urban environment

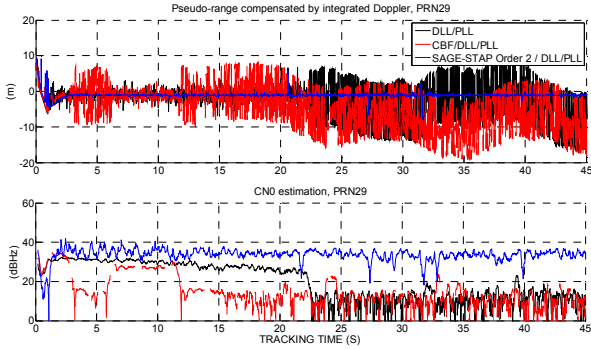


Fig. 7: Pseudo range compensated by integrated Doppler (CCD) and C/N0 for the PRN 29 in urban environment

Table. 2: standard deviation of the CCD averaged on all the tracked satellites in an urban environment

Algorithms	σ (m)
DLL/PLL	13
CBF/DLL/PLL	13.5
SAGE/DLL/PLL Order 2	0.7

4. SIMULATION RESULTS IN A MULTI-FREQUENCY CONTEXT

In the multi-frequency processing, the algorithms first have to be analyzed based on numerical simulations before being tested on real world data. From the state of the art on multi-frequency processing adapted to the multipath mitigation, we selected one method: the algorithm presented in [7] which assumes uncorrelated multipath between the two bands (here E5A and E5b). this algorithm is compared to the adaptation of the SAGE/STAP algorithm in the multi-frequency context presented in sub-section 2.3. For the channel environment simulation, we use the Simplified Channel for Urban Navigation (SCHUN) generator [17]. At the output of the SCHUN simulator, all the paths (LOSS and MP) are defined with a complex amplitude, delay, Doppler, and DOA every 20ms (thus, the paths parameters are assumed static during 20ms). For each path, we generated a BPSK(10) modulation sampled at $f_s = 20\text{MHz}$, and we summed all the signal components as in (1). Note that the number of multipath may be very large (> 4000). An additive white noise random process with a power of -128.9dBW (for each band) is used for the baseband signal generation. Note that SCHUN does neither model the

atmospheric effects nor the RF distortions. Thus, no inter-band delay is generated in this simulation.

The scenario simulated by SCHUN is represented in Fig. 8, and the total narrow band power time series for each band are plotted in Fig 9. The speed of the receiver is equal to 5m/s during 10s . Thus, the sampling distance is equal to 0.1m on a 50m linear trajectory. At the beginning of the simulation, the satellite range, azimuth and elevation are respectively 19986km , 45° and 35° (the x and y axis are respectively orthogonal and parallel to the canyon direction).

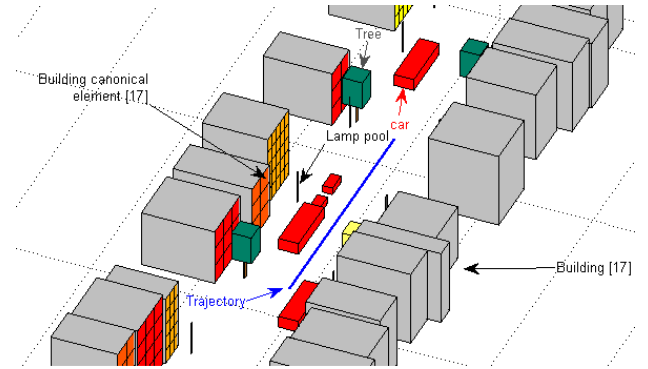


Fig. 8: Multi-frequency environment generated by SCHUN

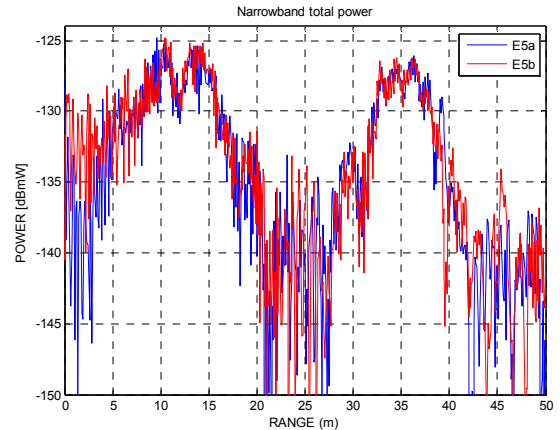


Fig. 9: Total narrow band power on E5a and E5b, SCHUN generation

Here, the loops parameters are the same as in section 3, except for the DLL bandwidth that is now 5Hz . The Figure 10 represents the tracking performances in term of pseudo-range error and Doppler error for each tracking algorithm. As expected, the multi-frequency processing provides better performance than mono frequency processing. From the table 3, which presents the pseudo-range error standard deviation computed from 0 to 40m of the simulated trajectory, the multi-frequency processing improves by more than a factor of 2 the code delay estimation. Thus, the multi-frequency processing reduces not only the noise error, but also a part of the multipath component.

In this scenario, the SAGE algorithm (based on a wideband view of the multi-frequency channel), provides better performance in terms of delay estimation than the

approach based on uncorrelated channels [7] (see Fig. 10 and table 3). Indeed, the assumption on the delay and the Doppler (section 1.3) provides redundancy which improves the reception of the LOS path.

Last, we can note a significant improvement of the SAGE approach in presence of strong fading events. After 40m, the receiver is in an NLOS situation, and the tested methods exhibit a loss of lock with the exception of the SAGE algorithm.

Table 3: Pseudo range error std from 0 to 40m, multi-frequency simulation

Algorithms	Pseudo range std
DLL/PLL (E5a)	2.8 m
DLL/PLL (E5a/E5b [7])	1.7 m
SAGE/DLL/PLL (E5a/E5b)	0,9 m

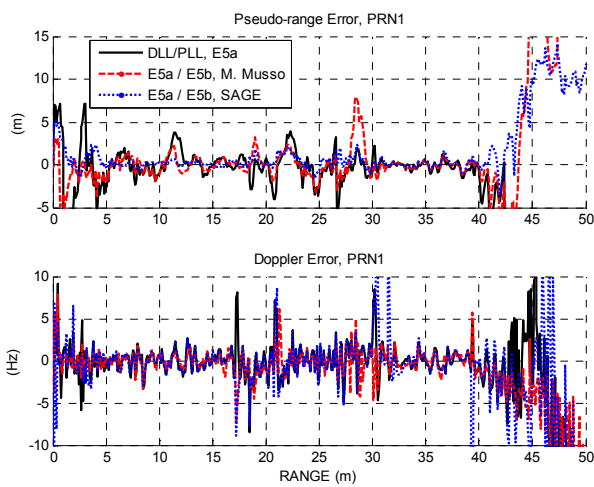


Fig. 10: Pseudo range and Doppler error, multi-frequency simulation

5. CONCLUSIONS

In this work we have addressed the problem of estimating the propagation time-delay of the LOS signal in a GNSS receiver under the presence of severe multipath. To reduce the influence of the multipath, we investigated the use of diversity algorithms. The diversity can either lie on the space domain (antenna diversity) or on the frequency domain (frequency band diversity). In both cases, the algorithms principle consists in taking benefit from the information redundancy given by diverse channels.

In a multi-antenna context, the algorithm and the associated performances have already been presented based on numerical simulations. This paper presents the validation of previous results based on real world data acquired with the CNES multi-antenna bit Grabber. The improvement of the pseudo range estimation in presence of multipath is better than a factor of 4 (with a 4 antenna array), which shows that the space diversity reduces not only the noise error, but also the MP error.

In a multi-frequency approach (here two frequencies E5a and E5b), the simulation based on the SCHUN simulator shows that multi-frequency processing is also a promising method for the multipath reduction, with a significant improvement in presence of fading events. However, two issues remain to be dealt with: first of all, the path delays between both bands are not the same due to the ionospheric effect and due to the RF stages. The algorithm performances degradation w.r.t. inter-band delay estimation is still to be characterized. Secondly, multi-frequency processing can lead to multi-modulation processing. The behaviour of the proposed method in the case of multi-modulation processing is still to be investigated.

Last but not least, as each diversity techniques provides promising results in terms of multipath mitigation, it should be interesting to investigate multi-antenna and multi-frequency processing in future works.

REFERENCES

- [1] A. J. Van Dierendonck, P. Fenton, and T. Ford, "Theory and Performance of Narrow Correlator Spacing in a GPS Receiver", Journal of the institute of navigation, vol.39, n°3, Fall 1992.
- [2] R. D. J. Van Nee, J. Sierveld, P. C. Fenton, and B. R. Townsend, "The Multipath Estimating Delay Lock Loop: Approaching Theoretical Accuracy Limits", IEEE Position, Location and Navigation Symposium, Las Vegas, Nevada, April U-15, 1994.
- [3] S. Rougerie, G. Carrie, L. Ries, F. Vincent, R. Pascaud, E. Corbel, M. Monnerat : "Multipath mitigation methods based on antenna array", Proc. ION ITM 2011, San Diego, CA, January 2011.
- [4] S. Rougerie, G. Carrie, F. Vincent, L. Ries, M. Monnerat , "A New Multipath Mitigation Method for GNSS Receivers based on an Antenna Array", International Journal of Navigation and Observation, vol. 2012. Paper ID 804732, 11 pages, 2012. doi:10.1155/2012/804732.
- [5] S. Rougerie: « Algorithme de diversité d'antennes appliqué à la réception des signaux GNSS en environnement urbain et sur terminal mobile ». Ph.D dissertation, ISAE 2012.
- [6] S. Rougerie, G. Carrie, L. Ries, F. Vincent, R. Pascaud, M. Monnerat : "A new sensor array receiver for multipath mitigation in GNSS", Proc. European Navigation Conference 2010, Braunschweig, Germany, October 2010.
- [7] M. Musso, G. Gera, A. Cattoni, and C. S. Regazzoni, "GNSS multifrequency receivers in urban environment: Theoretical analysis," in Proceedings of ION GNSS 2005, Long Beach Convention Center, CA, sep 2001, pp. 2661–2669.

- [8] N. I. Ziedan, "Multi-frequency combined processing for direct and multipath signals tracking based on particle filtering," in Proceedings of ION GNSS 2011, Portland, OR, 2011, pp. 1090– 1101.
- [9] J. Israel, G. Carrie, M. Ait-Ighil, "A Wideband and Multifrequency GNSS Propagation Channel Simulation", Proc. First CNES-ONERA Workshop on Earth-Space Propagation, 21 to 23 January 2013, ONERA, Toulouse, France.
- [10] J. Israel, G. Carrie, M. Ait-Ighil, "A Wideband and Multifrequency Propagation Channel Simulation", Proc. 7th European Conference on Antennas and Propagation (EuCAP), 2013, Gothenburg, Sweden, April 2013.
- [11] H. Akaike, "Information theory and an extension of the maximum likelihood principle", In Petrov, B. and Csaki, F., editors, 2nd International Symposium on Information theory, pp 267-281, Budapest, Hungary.
- [12] G. Carrie, F. Vincent, T. Deloues, D. Pietin, A. Renard, F. Letestu : "Optimal STAP Algorithms to GNSS Receivers", Proc. European Navigation Conference 2006, May 2006, Manchester International Convention Centre.
- [13] A. Jeffrey: « Space-Alternating Generalized Expectation Maximization Algorithm ». IEEE on signal processing, Vol 42, N° 10, October 1994.
- [14] F. Antreich: "Array Processing and Signal Design for Timing Synchronization", Ph.D dissertation, Munchen Tech, 2011.
- [15] G. Carrie: "techniques d'antennes adaptatives pour récepteurs de radionavigation par satellites résistants aux interférences", Ph.D dissertation, ISAE 2006.
- [16] E. D. Kaplan: "Understanding GPS, Principles and Applications", Artech House, Second Edition.
- [17] M. Ait Ighil: "Enhanced physical-statistical simulator of the land mobile satellite channel for multipath modelling applied to satellite navigation systems", Ph.D dissertation, ISAE 2013.